

about four orders of magnitude thus requiring seed masses of the order $10^5 M_\odot$ (Shapiro 2005)

The formation of such massive seeds has been considered in the context of the direct collapse mode here gas in a 10^7 – $10^8 M_\odot$ halo is expected to collapse without fragmentation into a single central object (Koushappas et al. 2004 Bege man et al. 2006 Lodato & Natarajan 2006 Spaans & Silk 2006 Voelter et al. 2008 Bege man & Shosman 2009) in order to avoid fragmentation molecular hydrogen needs to be efficiently dissociated requiring a strong ambient UV field (Omukai 2001 Bromm & Loeb 2003 Shang et al. 2009 Scherer et al. 2010 Latif et al. 2011 Van Borm & Spaans 2013) Such radiation backgrounds may have been provided by nearby starburst galaxies which may indeed occur frequently enough to explain the observed abundance of SMBHs at $z \sim 6$ (Dijkstra et al. 2008 Agar et al. 2012)

Using numerical simulations see et al. (2008) have modeled the gravitational collapse of massive primordial halos cooling via atomic hydrogen reporting an isothermal density profile and angular momentum transport via bar-ke instability during the formation of the first peak Regan & Haehnelt (2009) presented the first study following the evolution beyond the first peak and modeling the formation of self-gravitating disks on parsec-scales here these studies employed a typical resolution of 16 cells per Jeans length thus as recently demonstrated that turbulent structures can only be resolved with a resolution of at least 32 cells per Jeans length preferably more (Sur et al. 2010 Federrath et al. 2011 Turk et al. 2012) in a set of high-resolution simulations following the formation of the first peak Latif et al. (2013a,b) found extended turbulent structures in the center of massive primordial halos but no signs of smped disks or bar-ke instability Disks do however form at later stages of the evolution with masses of $\sim 1000 M_\odot$ on scales of 30 AU and characteristic accretion rates of $\sim 1 M_\odot \text{ yr}^{-1}$ (Latif et al. 2013c) As a result very massive central objects may indeed form in rather short cosmic times The dynamical times have a so been explored by Ho et al. (2013) finding a somewhat different result indicating the formation of toroidal structures on scales of several parsecs thus however not fully clear to

which extent the latter is a result of the smped initial conditions employed in the calculation in order to provide more quantitative predictions regarding the conditions here black holes may form Preto et al. (2013) explored the correlations of the baryon spin with the spin of the dark matter showing that the resulting correlation is however weak and that the baryon properties cannot be naively extrapolated from the dark matter

here the accumulation of high masses seems feasible from a hydrodynamical point of view the resulting objects still considerably more uncertain As a first step we expect the formation of a massive protostar as the gas becomes optically thick at high densities (Omukai & Palla 2001 2003 Hosokawa et al. 2012a) thus however unclear how these objects are going to evolve and whether they form a supermassive star or a quas-star here a supermassive star denotes a conventional star with very high masses of 10^3 – $10^6 M_\odot$ (Shapiro & Teukosky 1986) a quas-star refers to an object with similar mass but here the central core has collapsed into a zero-mass black hole (Bege man et al. 2006 Bege man 2010) The latter then

accretes mass from the stellar envelope here the quas-star as a whole may accrete at a rate larger than the Eddington rate of the black hole A central question however concerns the conditions under which we expect the formation of a quas-star as opposed to a supermassive star and which of these objects should be expected as the generic outcome in the context of the direct collapse mode Also the properties of these objects are of high interest as the amount of stellar feedback may influence the final accretion rates

In order to explore that question Hosokawa et al. (2012a) recently followed the evolution of rapidly accreting protostars showing that they expand as cool supergiants thus inhibiting the feedback from accretion luminosity and potentially allowing accretion to proceed for very long times Hosokawa et al. also found that nuclear burning starts at stellar masses of about $\sim 50 M_\odot$ and simultaneously the end of the calculation at $10^3 M_\odot$ Therefore the remainder indicates no transition towards a quas-star at least during the evolutionary phase considered thus however important to assess how long this phase of efficient accretion can be maintained and under which conditions a transition to a supermassive main-sequence star can be expected which can potentially influence the accretion flow via radiative feedback (Omukai & Nutsuka 2002 Johnson et al. 2011 2012) here the majority of such supermassive stars directly collapse into a black hole (Fryer & Heger 2011) a small mass window exists around $55000 M_\odot$ here violent supernova explosions of up to 10^{55} erg may occur (Johnson et al. 2013)

Following a different approach Bege man et al. (2006) and Bege man (2010) have proposed the formation of a black hole in the interior of rapidly accreting objects leading to quas-stars as the progenitors of SMBHs Bege man et al. (2006) argued that for quas-stars with 10^4 – $10^5 M_\odot$ the typical accretion timescales are considerably shorter than the timescale for nuclear burning and as a result the latter may not be able to stop the collapse of the central core A potential advantage of such a configuration is that the accretion onto the central object is limited by the Eddington accretion rate of the black hole but by the Eddington accretion rate of the more massive quas-star (Bege man et al. 2008) Bege man (2010) considers objects with more than $10^6 M_\odot$ which first evolve towards the main sequence as a supermassive star but then form a black hole after an extended phase of nuclear burning Ba et al. (2011) followed the evolution of black holes in a quas-star employing the ambdrge STARS stellar evolution package (Eggleton 1971 Pols et al. 1995) finding that the black hole may efficiently accrete 10% of the stellar mass before hydrostatic equilibrium breaks down They also report that the results are sensitive to the boundary conditions in the interior The contraction of an embedded isothermal core in a stellar envelope as further explored by Ba et al. (2012) in the framework of the Schönberg–Kandrasekhar limit

here the models for the quas-stars typically employed a Thompson-scattering opacity Hosokawa et al. (2012a) reported that H^- rather than Thomson scattering dominates the opacity in the protostellar atmosphere They find luminosity close to the Eddington luminosity

$$L_{\text{Edd}} = \frac{4\pi GMm_p c}{\sigma_T} = 3.8 \times 10^4 L_\odot \left(\frac{M}{M_\odot} \right), \quad (1)$$

where G is the gravitational constant m_p the proton mass c the speed of light σ_T the Thomson scattering cross section

on and M the mass of the star. The temperatures in the atmosphere are rather cool ~ 5000 K as the protostars are on the Hayash track. As a result the characteristic radii evolve as

$$R_{ini} = 2.6 \times 10^2 R_{\odot} \left(\frac{M}{M_{\odot}} \right)^{1/2}. \quad (2)$$

The protostars are thus considerably more extended and show an increasing stellar radius as a function of mass. Here the models of Begeelman et al. (2006) and Begeelman (2010) indicate a constant radius as a function of stellar mass. The difference is crucial as the stellar radius regulates the temperature on the surface and thus the strength of protostellar feedback. In fact the behavior reported by Hosokawa et al. (2012a) is well-known in cases where the accretion timescale

$$t_{acc} = \frac{M}{\dot{M}}, \quad (3)$$

is much smaller than the Kelvin-Helmholtz timescale

$$t_{KH} = \frac{GM^2}{RL}. \quad (4)$$

However, Hosokawa et al. (2012a) report that this behavior extends into the regime where $t_{KH} < t_{acc}$ where Kelvin-Helmholtz contraction is faster than mass growth via accretion. The physical mechanisms which allow this phase to continue are discussed in detail in section 2. Taking the maximum luminosity of the star

$$L_{max} \sim 0.6 L_{\odot} \left(\frac{M}{M_{\odot}} \right)^{11/2} \left(\frac{R}{R_{\odot}} \right)^{-1/2}, \quad (5)$$

which assumes Kramer's opacity $\kappa \propto \rho T^{-3/5}$ (Hayash et al. 1962) and an initial radius as given in Eq. (2) they show that both timescales are equal at protostellar masses of

$$M_{eq} = 14.9 M_{\odot} \left(\frac{\dot{M}}{0.01} \right)^{0.26}, \quad (6)$$

here we parametrized the accretion rate as $\dot{M} \equiv \dot{m} M_{\odot} \text{ yr}^{-1}$. On the other hand, the accreting star remains on the Hayash track up to stellar masses of $1000 M_{\odot}$, the highest mass reached in the calculation of Hosokawa et al. (2012a). The extended envelope locked at $T_{\text{eff}} \sim 5000$ K allows efficient accretion through moderate feedback for a longer period.

In this paper we aim to assess how long this efficient accretion phase can be maintained beyond $M \sim 1000 M_{\odot}$ without strong feedback from the protostar in addition we

discuss the potential impact of nuclear burning for the evolution of the accreting objects and the conditions under which a quasi-star as opposed to a supermassive star may form. For this purpose we explore the interplay of mass accretion and Kelvin-Helmholtz contraction in section 2. We calculate the impact of nuclear burning in section 3. A final discussion of our results is provided in section 4. The impact of additional processes such as deuterium shell burning and hydrogen burning via the pp-chain is assessed in the appendix.

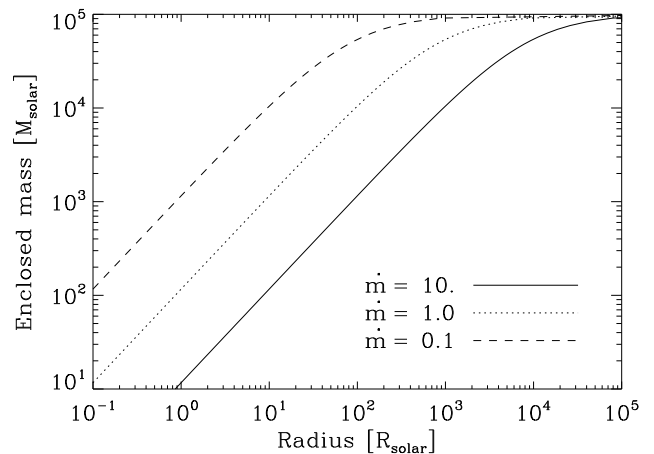


Fig. 1. The enclosed mass as a function of radius in the protostar calculated from Eq. (10), assuming a total stellar mass of $10^5 M_{\odot}$ and mass accretion rates $\dot{m} = 0.1, 1, 10$. The current time t is calculated as $t = (M/M_{\odot})/\dot{m}$. For a given mass shell, larger accretion rates imply larger radii, as the star had less time to contract.

2. The interplay of mass accretion and Kelvin-Helmholtz contraction

In the following we sketch why the protostar may maintain a large envelope even if the Kelvin-Helmholtz timescale becomes shorter than the timescale for accretion. For this purpose we consider mass shells of enclosed mass M located at radius $R(M, t)$. A mass shell M forms at the time M/\dot{M} through a radius as given by Eq. (2). The radius of these mass shells evolves on the Kelvin-Helmholtz timescale given as

$$t_{KH}(M, R) = \frac{GM^2}{R(M, t)L_{\text{Edd}}}. \quad (7)$$

As a result we have

$$\frac{dR}{dt} = -\frac{R(M, t)}{t_{KH}(M, R)}. \quad (8)$$

The equation is integrated between the initial radius R_{ini} when the mass shell forms given in (2) corresponding to the time $t_{ini}(M) = M/\dot{M}$ to the current radius R at time t . The integration yields

$$\frac{1}{R} = \frac{1}{R_{ini}} + \frac{4\pi m_p c}{\sigma_T M} (t - t_{ini}(M)). \quad (9)$$

Inserting the initial radius as given in Eq. (2) and expressing the result in astrophysical units we obtain

$$\frac{1000 R_{\odot}}{R} = \frac{1000 R_{\odot}}{2.6 \times 10^2 (M/M_{\odot})^{1/2}} + \frac{1.04 \text{ yr}^{-1} (t - t_{ini}(M))}{M/M_{\odot}}. \quad (10)$$

The first term on the right-hand side thus dominates right after the formation of a mass shell and determines its initial radius. Here the second term describes its evolution due to Kelvin-Helmholtz contraction. It is remarkable that at late

times the second term dominates and the evolution of the radius appears to be independent of the initial position. This can be understood as our expression for the Kelvin-Helmholtz timescale Eq. (7) scales with the inverse radius of the mass shell. As a result the evolution slows down during the contraction implying that the Kelvin-Helmholtz timescale may increase significantly in the interior. An example for the resulting structure in a $10^5 M_\odot$ star is given in Fig. 1 including both the regime where the first and the second term of the equation dominate.

One can estimate when a given mass shell reaches the densities of nuclear burning which we take as $\rho_{nuc} \sim 1 \text{ g cm}^{-3}$ (Hosokawa et al. 2012a) to obtain a radius of nuclear burning which is given as

$$R_{nuc} = \left(\frac{3M}{4\pi\rho_{nuc}} \right)^{1/3} \sim 1.2R_\odot \left(\frac{M}{M_\odot} \right)^{1/3}. \quad (11)$$

A comparison with Eq. (2) shows that this radius always remains smaller than the radius of the star by at least a factor of 1000 and in fact increases more gradually with stellar mass. A given mass shell M only reaches nuclear densities on timescales much longer than the Kelvin-Helmholtz timescale t_{KH} which increases as R^{-1} and can thus determine the time when nuclear densities are reached by equating (11) with the second term in (10). As a result one obtains

$$\Delta t = t - t_{ini}(M) = 710 \text{ yrs} \left(\frac{M}{M_\odot} \right)^{2/3}. \quad (12)$$

During the time interval Δt the star accretes an additional mass $\Delta M = \dot{M}\Delta t$ considering a given mass shell one can calculate the ratio

$$\frac{\Delta M}{M} = \frac{\dot{M}\Delta t}{M} \sim 710\dot{m} \left(\frac{M}{M_\odot} \right)^{-1/3}, \quad (13)$$

which describes how much additional mass is accreted before the shell reaches nuclear densities. The ratio drops below 1 only for protostellar masses of

$$M \geq 3.6 \times 10^8 \dot{m}^3 M_\odot. \quad (14)$$

For typical accretion rates of $\dot{m} \sim 10^{-3}$ this happens already at mass scales of order unity, thus transition occurs only at substantially larger masses above $1000 M_\odot$ for $\dot{m} > 10^{-2}$. Here a given shell evolves towards nuclear densities the amount of additional mass that is accreted is thus substantially higher than the mass in that shell. From Eq. (12) one can further derive the mass in the nuclear core in the limit that $t \gg t_{ini}(M)$ one obtains

$$M_{nuc} = \left(\frac{t}{710 \text{ yr}} \right)^{3/2} M_\odot = t_{710}^{3/2} M_\odot, \quad (15)$$

where we defined $t_{710} = t/(710 \text{ yr})$. As we neglected the term M/\dot{M} in Eq. (12) one notes that the derivation here implicitly assumes a sufficient mass supply to the protostar in order to feed the core, early in this approximation breakdown at the mass scale derived in (14). At that point both the protostellar mass as well as the mass in the nuclear core may become approximately constant and we expect a transition towards supermassive main sequence stars.

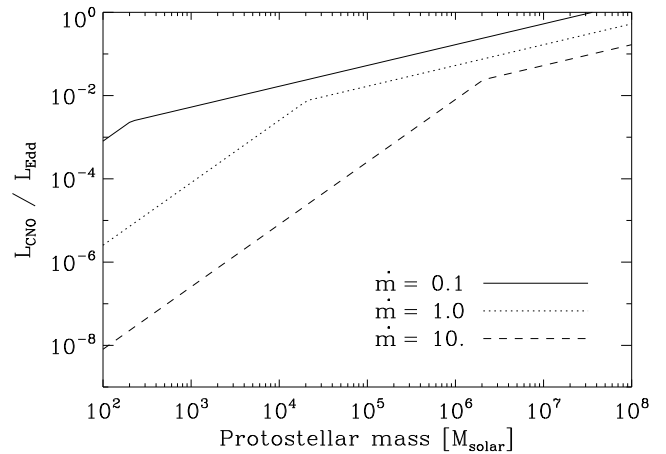


Fig. 2. The ratio of nuclear luminosity provided via the CNO-cycle over the Eddington luminosity of the star (A.5) as a function of protostellar mass for different mass accretion rates. The CNO luminosity is calculated here as the minimum of the estimate in Eq. (24) and the Eddington luminosity of the nuclear core (25). At high protostellar masses, one can clearly recognize the transition to the regime where nuclear burning is limited by the Eddington luminosity of the core. Larger accretion times imply that less time was available for contraction, thus reduced nuclear luminosities.

From this model one readily obtains a set of relevant conclusions concerning the evolution of the protostar in particular if the accretion rate is high, a substantial amount of additional matter is accreted before a given shell reaches nuclear densities. As a result the evolution of the protostar is dominated not by the interior shell but by the additional matter which is accreted during the contraction. This behavior only changes when the timescale of accretion becomes comparable to the timescale on which the outer mass shells are able to reach nuclear densities. As we show here the latter is significantly larger than the Kelvin-Helmholtz timescale of the star and scales with the R_{nuc}^{-1} . The transition occurs when a critical mass scale of $3.6 \times 10^8 \dot{m}^3 M_\odot$ is reached, implying a transition towards supermassive main sequence stars. One notes that the transition may even occur earlier if \dot{m} decreases with time.

3. The nuclear evolution

In this section we assess the potential role of nuclear burning. For this purpose we show that the transition to the NO-cycle rapidly occurs and regulates the production of helium in the nuclear core. We then calculate under which conditions the fuel in the nuclear core is exhausted, here the protostar manifests its extended envelope. The latter implies the potential formation of a black hole in the interior, thus a transition into a quasistar.

3.1. Importance of the CNO-cycle

Here the pp-cycle dominates in the very beginning (see appendix x) we show here that the transition to the NO-cycle rapidly occurs as a result of helium burning via the $\text{tr p}-\alpha$ process. Following Padmanabhan (2000) the en-

energy production rate via the $\text{p}-\alpha$ reaction given as

$$\epsilon_{3\alpha} = \frac{5.1 \times 10^8 \rho^2 Y^3}{T_9^3} e^{-4.4027/T_9} \text{ erg g}^{-1} \text{ s}^{-1}, \quad (16)$$

here $Y \sim 0.25$ denotes the mass fraction of helium and T_9 denotes the gas temperature in units of 10^9 K. It is straightforward to check that the energy production rate changes by several orders of magnitude for temperature changes of the order 10%. As shown by Hosokawa et al. (2012a) the highest temperatures with $T_9 \sim 0.15$ are expected in the center of the nuclear core which has an enhanced nuclear density of 10 g cm^{-3} and a volume filling factor $\epsilon_{\text{fill}} \sim 0.01 - 0.1$. The contribution of that region to the helium burning is significant due to the steep temperature dependence. For the following estimates we assume that efficient mixing occurs throughout the nuclear core implying that the heavy elements produced in the central region are available throughout the core. On the other hand mixing is inefficient nuclear burning via the NO cycle dominates even more in the central region due to its higher metallicity.

Noting that the energy released by a single $\text{p}-\alpha$ reaction corresponds to 1.166×10^{-5} erg the heavy element production rate per unit volume is given as

$$n_{3\alpha} = \frac{\epsilon_{3\alpha}}{1.166 \times 10^{-5} \text{ erg}}. \quad (17)$$

The NO mass in the core thus evolves as

$$\dot{M}_{\text{CNO}} = \dot{n}_{3\alpha} \epsilon_{\text{fill}} M_{\text{nuc}} \times 12 m_p, \quad (18)$$

and an integration yields

$$M_{\text{CNO}} = 7.1 \times 10^{-17} \epsilon_{\text{fill}}^2 t_{710}^{5/2} M_{\odot}. \quad (19)$$

Assuming efficient mixing the resulting metallicity in the nuclear core is then

$$Z = \frac{M_{\text{CNO}}}{M_{\text{nuc}}} = 6.3 \times 10^{-9} t_{710} \epsilon_{\text{fill}}. \quad (20)$$

We recall that the energy production rate in the NO cycle is given as (Padmanabhan 2000)

$$\epsilon_{\text{CNO}} = \frac{4.4 \times 10^{25} \rho X Z}{T_9^{2/3}} e^{-15.228/T_9^{1/3}} \text{ erg g}^{-1} \text{ s}^{-1}. \quad (21)$$

Since the energy production rate depends sensitively on the temperature we expect its contribution in the innermost core to be dominant. For the temperature $T_9 = 0.15$ it is straightforward to show that energy production via the NO cycle becomes comparable to the pp cycle for a metallicity of $Z_c = 2 \times 10^{-12}$. A comparison with Eq. (20) shows that the NO cycle thus dominates after a short time of

$$t_{\text{CNO}} = 2.25 \epsilon_{\text{fill},-1}^{-1} \text{ yr}, \quad (22)$$

where we introduced $\epsilon_{\text{fill}} = 0.1 \epsilon_{\text{fill},-1}$. We note here that this timescale is probably not accurate as our assumptions in section 2 (in particular concerning the Eddington luminosity) only become valid at later times. Nevertheless this result implies that the NO cycle can be expected to be relevant early on and thus needs to be considered. As the production of elements becomes increasingly efficient at late times we expect that the expression (20) yields a reasonable estimate in the period of interest

with the above assumptions the NO luminosity due to nuclear burning is given as

$$L_{\text{CNO}} = \epsilon_{\text{CNO},Z_c} \left(\frac{Z}{Z_c} \right) M_{\text{nuc}} \epsilon_{\text{fill}}, \quad (23)$$

where $\epsilon_{\text{CNO},Z_c}$ denotes the energy production rate via the NO cycle evaluated at the critical metallicity Z_c using Eq. (20) is obtained

$$L_{\text{CNO}} = 1.3 \times 10^5 \epsilon_{\text{fill}}^2 t_{710}^{5/2} L_{\odot}. \quad (24)$$

The Eddington luminosity of the nuclear core is given as

$$L_{\text{Edd,core}} = 3.8 \times 10^4 \dot{m} t_{710}^{3/2} L_{\odot}. \quad (25)$$

The ratio of these luminosities to the Eddington luminosity of the star is given in Fig. (2). Even here the luminosity produced by nuclear burning approaches the Eddington luminosity of the star only around stellar masses of $10^8 M_{\odot}$ implying no relevant impact on the stellar evolution during the earlier stages. A comparison of these expressions yields the timescale

$$t_c = 2.1 \times 10^4 \epsilon_{\text{fill},-1}^{-2} \text{ yr}. \quad (26)$$

For $\epsilon_{\text{fill},-1} \sim 1$ as indicated by Hosokawa et al. (2012a) for $\dot{m} = 0.1$ the NO luminosity would exceed the Eddington luminosity of the core after $\sim 2 \times 10^4$ yr shortly after the end of the r-process. However when the Eddington luminosity is reached one would expect an expansion of the nuclear core implying lower densities and an adiabatic decrease in temperature. Due to this thermostat it is likely that the core adjusts to a state maintaining its Eddington luminosity.

We do not demonstrate that the nuclear core is not converted to helium before the critical timescale t_c after which the core radiates at its Eddington luminosity. We consider the production of helium by the NO process given as

$$\dot{N}_{\text{He,CNO}} = \frac{L_{\text{CNO}}}{4.3 \times 10^{-5} \text{ erg}}, \quad (27)$$

and the helium mass production rate

$$\dot{M}_{\text{He,CNO}} = 12 m_p \times \dot{N}_{\text{He,CNO}}. \quad (28)$$

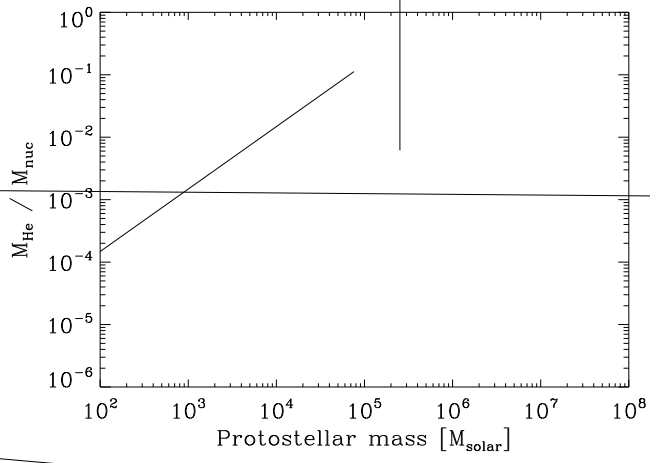
An integration yields

$$M_{\text{He,CNO}} = 1.0 \times 10^{-3} \epsilon_{\text{fill}}^2 t_{710}^{7/2} M_{\odot}. \quad (29)$$

A comparison with the mass of the core indicates that they become comparable at

$$t_{\text{He,CNO}} = 2.25 \times 10^5 \epsilon_{\text{fill},-1}^{-1} \text{ yr}, \quad (30)$$

implying that a pure helium core can only be formed once the nuclear luminosity is equal to the Eddington luminosity of the core.



scales based on the reasonable assumption that the luminosity of the core is given by its Eddington luminosity in agreement with the numerical results by Hosokawa et al. (2012a). Uncertainties are however present as our calculation for the evolution of the core mass assumes that the luminosity of each mass shell is given by the Eddington luminosity. Following Hosokawa et al. (2012a) the latter is a good but not precise approximation. Further corrections can be expected in particular when approaching nuclear densities when feedback from nuclear burning becomes significant. Additional effects could be introduced as a result of rotation which has not included in this model. We thus expect our results to provide an order of magnitude estimate for the critical accretion rate which may be determined more accurately employing stellar evolution calculations but also a more realistic mode for the time-dependent accretion rate. We also note here that Hosokawa et al. (2012a) reported a slight dependence of the results on the employed boundary conditions for the protostar. In the remaining calculations adopted shock boundary conditions they also explored the effect of differential accretion provided by photospheric boundary conditions. In that case a slightly higher accretion rate of $0.3 M_{\odot} \text{ yr}^{-1}$ appears to be required to maintain the extended envelopes but the overall evolution remains very similar.

For comparison we note that recent simulations by Latif et al. (2013c) reported accretion rates of $\sim 1 M_{\odot} \text{ yr}^{-1}$ in halo with $\sim 10^7 M_{\odot}$. Adopting a constant accretion rate the transition to a supermassive main sequence star would occur at a stellar mass of $3.6 \times 10^8 M_{\odot}$. As the nuclear fuel is however exhausted earlier a black hole may form before this transition giving rise to an evolution as sketched by Baetens et al. (2011). However due to the limited gas reservoir and as here the halo mass is in fact comparable to the mass scale of the corresponding quasars it seems likely that the accretion rate substantially decrease at late times implying that the transition towards the supermassive star should occur at an earlier stage which is then determined by the time evolution of the accretion rate and that supermassive stars with $10^4 - 10^5 M_{\odot}$ might be the most generic outcome of the collapse. More massive objects appear to be possible at least in principle if a larger gas reservoir is available in more massive dark matter halos. In order to assess the potential influence of rotation we estimated the amount of rotational support in the central $10^3 M_{\odot}$ clumps reported by Latif et al. (2013c) which varied between 5–20% in different simulations. The densities of $\sim 10^{-10} \text{ g cm}^{-3}$ these are still orders of magnitude below the characteristic densities in the protostar such that we cannot yet draw strong conclusions regarding the final amount of rotational energy. However we note that Stacy et al. (2012) reported a significant amount of rotation in primordial protostars based on numerical simulations of Greif et al. (2012) and a quite similar case can be expected here. As recently shown by Reisswig et al. (2013) the latter may have a substantial impact on the collapse of supermassive stars implying the potential formation of a black hole binary and a subsequent merger accompanied with efficient emission of gravitational waves. The latter provides a potential pathway of probing black hole formation scenarios with LISA¹ in a narrow mass range around $\sim 55000 M_{\odot}$.

one may further expect the occurrence of highly energetic supernovae with energies up to 10^{44} erg which can be potentially detected with JST² (Johnson et al. 2013).

Returning to the fate of supermassive stars the re-evolution in the presence of UV feedback as assessed by Omukai & Nutsuka (2002) and Johnson et al. (2012) in the case of spherical symmetry. These authors find that UV feedback is unable to stop accretion for rates above $\sim 0.1 M_{\odot} \text{ yr}^{-1}$. As a result the expected stellar masses

$$M_{\text{UV}} \sim 10^3 M_{\odot} \left(\frac{\dot{m}}{10^{-3}} \right)^{8/7}. \quad (36)$$

For accretion rates of $\sim 0.1 M_{\odot} \text{ yr}^{-1}$ our results exceed this value as the protostars remain on the Hayashi track up to a mass of $\sim 3 \times 10^5 M_{\odot}$ making feedback inefficient. Therefore taking protostellar evolution into account favours the formation of more massive objects in cases a critical question concerns the time evolution of the accretion rate since the transition to supermassive stars is regulated by the accretion rate at late times. In this paper we provide a first assessment for the case of constant accretion rates and spherical symmetry the potential implications of time-dependent accretion rates need to be addressed in more detail in the future along with the implications of rotation during protostellar evolution.

Acknowledgements. DRGS and ML thank for funding from the Deutsche Forschungsgemeinschaft (DFG) via the SFB 477/A “Astrophysical instabilities and turbulence” project A. DRGS further acknowledges financial support via the Schwerpunktprogramm SPP 1355 “Physics of the Interstellar Medium” under grant SCHL 477/A. DRGS and FP acknowledge the financial support of PRIN INAF “The Formation of Stars”.

References

- Abe, T., Bryan, G. L., Norman, M. L., Science, ,
 Agarwa, B., Khochfar, S., Johnson, J. L., et al., MNRAS, ,
 Ba, , H., Tout, C. A., ytow, A. N., MNRAS, ,
 Ba, , H., Tout, C. A., ytow, A. N., Eddridge, J. J., MNRAS, ,
 Begean, M. C., MNRAS, ,
 Begean, M. C., Rossi, E. M., Armitage, P. J., MNRAS, ,
 Begean, M. C., Shostan, I., ApJ, , L
 Begean, M. C., Conteri, M., Rees, M. J., MNRAS, ,
 Bro, , Larson, R. B., ARA A, ,
 Bro, , Loeb, A., ApJ, ,
 Choi, J. H., Shostan, I., Begean, M. C., ArXiv e prints
 Car, P. C., Glover, S. C. O., Kessen, R. S., ApJ, ,
 Car, P. C., Glover, S. C. O., Sith, R. J., et al., Science, ,
 Devecchi, B., Conteri, M., ApJ, ,
 Devecchi, B., Conteri, M., Coppi, M., Haardt, F., MNRAS, ,
 Devecchi, B., Conteri, M., Rossi, E. M., Coppi, M., Portegies Zwart, S., MNRAS, ,
 Dijstra, M., Haihan, Z., Mesinger, A., Witte, S., ArXiv e prints
 Doppe, G., Glover, S. C. O., Car, P. C., Kessen, R. S., ApJ, , L
 Doppe, G., Glover, S. C. O., Car, P. C., Kessen, R. S., ArXiv e prints
 Eggerton, P. P., MNRAS, ,
 Fan, X., Hennawi, J. F., Richards, G. T., et al., AJ, ,

¹ LISA webpage: <http://lisa.nasa.gov/>

² JWST webpage: <http://www.jwst.nasa.gov/>

Fan, X., Strauss, M. A., Richards, G. T., et al. (2017), *ApJ*, 845, 101
 Fan, X., Strauss, M. A., Schneider, D. P., et al. (2018), *ApJ*, 861, 101
 Fan et al. (2019), *ApJ*, 881, 101
 Federrath, C., Sur, S., Schaeicher, D. R. G., Banerjee, R., Klessen, R. S., & ApJ, 845, 101
 Fryer, C. L., Heger, A., & Astronomische Nachrichten, 338, 101
 Fryer, C. L., Woosley, S. E., Heger, A., & ApJ, 600, 101
 Greif, T. H., Bromberg, J., Carilli, P. C., et al. (2015), *MNRAS*, 450, 101
 Greif, T. H., Springel, V., Hite, S. D. M., et al. (2016), *ApJ*, 820, 101
 Hai an, Z., & New A Rev., 15, 101
 Hayashi, C., Hoshi, R., Sugimoto, D., & Progress of Theoretical Physics Supplement, 152, 101
 Heger, A., Woosley, S. E., & ApJ, 600, 101
 Hosokawa, T., Oyaiki, K., & ApJ, 780, 101
 Hosokawa, T., Oyaiki, K., Yoroi, H., et al. (2017), *ApJ*, 845, 101
 Hosokawa, T., Oyaiki, K., Yoshida, N., Yoroi, H., & Science, 355, 101
 Hosokawa, T., Yoshida, N., Oyaiki, K., Yoroi, H., & ApJ, 845, 101
 Johnson, J. L., Khochfar, S., Greif, T. H., Durier, F., & MNRAS, 450, 101
 Johnson, J. L., Haehnelt, D. J., Even, S., et al. (2016), *ArXiv e-prints*, 1608.07552
 Johnson, J. L., Haehnelt, D. J., Fryer, C. L., Li, H., & ApJ, 820, 101
 Klessen, R. S., Glover, S. C. O., Carilli, P. C., & MNRAS, 450, 101
 Koushiappas, S. M., Bouc, J. S., Deere, A., & MNRAS, 450, 101
 Latif, M. A., Schaeicher, D. R. G., Schindt, R., Nieppel, J., & ArXiv e-prints, 1608.07552
 Latif, M. A., Schaeicher, D. R. G., Schindt, R., Nieppel, J., & MNRAS, 450, 101
 Latif, M. A., Schaeicher, D. R. G., Schindt, R., Nieppel, J., & MNRAS, 450, 101
 Latif, M. A., Schaeicher, D. R. G., Spaans, M., Zaroubi, S., & A&A, 599, 101
 Lodato, G., Natarajan, P., & MNRAS, 450, 101
 Misosavljević, M., Bromberg, J., Couch, S. M., & Oh, S. P., & ApJ, 845, 101
 Misosavljević, M., Couch, S. M., Bromberg, J., & ApJ, 845, 101
 Mortlock, D., & Nature, 461, 101
 Oyaiki, K., & ApJ, 845, 101
 Oyaiki, K., & ArXiv e-prints, 1608.07552
 Oyaiki, K., Inutsuka, S. I., & MNRAS, 450, 101
 Oyaiki, K., Palla, F., & ApJ, 845, 101
 Oyaiki, K., Palla, F., & ApJ, 845, 101
 Oyaiki, K., Schneider, R., Hai an, Z., & ArXiv e-prints, 1608.07552
 Oyaiki, K., Tsuribe, T., Schneider, R., Ferrara, A., & ApJ, 845, 101
 Padanabhan, T., & Theoretical Astrophysics, 101, 101
 Poels, O. R., Tout, C. A., Eggleton, P. P., Han, Z., & MNRAS, 450, 101
 Prieto, J., Jinenz, R., Hai an, Z., & ArXiv e-prints, 1608.07552
 Rees, M. J., & ARAA, 55, 101
 Regan, J. A., Haehnelt, M. G., & MNRAS, 450, 101
 Reisswig, C., Ott, C. D., Abdia, A. A., et al. (2016), *ArXiv e-prints*, 1608.07552
 Schaeicher, D. R. G., Spaans, M., Glover, S. C. O., & ApJL, 845, 101
 Schneider, R., Ferrara, A., Satvatter, R., Oyaiki, K., Bromberg, J., & Nature, 543, 101
 Schneider, R., Oyaiki, K., Bianchi, S., & MNRAS, 450, 101
 Schneider, R., Oyaiki, K., Longi, M., et al. (2016), *MNRAS*, 450, 101
 Shang, C., Bryan, G. L., Hai an, Z., & MNRAS, 450, 101
 Shapiro, S. L., & ApJ, 845, 101
 Shapiro, S. L., Teusler, S. A., & Bac Ho, S., & White Dwarfs and Neutron Stars: The Physics of Compact Objects
 Saitoh, R. J., Glover, S. C. O., Carilli, P. C., Greif, T., & Klessen, R. S., & MNRAS, 450, 101
 Saitoh, R. J., Hosokawa, T., Oyaiki, K., Glover, S. C. O., & Klessen, R. S., & MNRAS, 450, 101
 Spaans, M., Si, J., & ApJ, 845, 101
 Stacy, A., Greif, T. H., Bromberg, J., & MNRAS, 450, 101
 Stacy, A., Greif, T. H., Bromberg, J., & MNRAS, 450, 101
 Sur, S., Schaeicher, D. R. G., Banerjee, R., Federrath, C., & Klessen, R. S., & ApJL, 845, 101
 Susa, H., & ArXiv e-prints, 1608.07552
 Tur, M. J., Abe, T., O'Shea, B., & Science, 355, 101
 Tur, M. J., Oishi, J. S., Abe, T., Bryan, G. L., & ApJ, 845, 101
 van Borstel, C., Spaans, M., & ArXiv e-prints, 1608.07552
 von der Linden, M., Bebovary, J., & Reports on Progress in Physics, 80, 101
 von der Linden, M., Lodato, G., Natarajan, P., & MNRAS, 450, 101
 von der Linden, M., Fryer, C. L., & ApJ, 845, 101
 Wise, J. H., Tur, M. J., Abe, T., & ApJ, 845, 101

Appendix A: Additional nuclear processes

In section 3.1 we have shown that the transition to the NO cycle rapidly occurs implying that the latter regulates the formation of a helium core as discussed in section 3.2. However, additional nuclear processes are expected to simultaneously occur which we discuss here for completeness in the two sub-sections below. We assess the role of deuterium shell burning as well as the impact of hydrogen burning via the pp-change during the stellar evolution showing that these processes only have a minor impact on the stellar evolution.

Appendix A.1: Deuterium burning

As reported by Hosokawa & Omukai (2009) deuterium shell burning may occur even before nuclear burning starts in the core. The luminosity from deuterium shell burning is given as

$$L_D = 1.5 \times 10^5 L_\odot \left(\frac{\dot{m}}{0.1} \right) \left(\frac{[D/H]}{2.5 \times 10^{-5}} \right), \quad (\text{A } 1)$$

where D/H denotes the deuterium abundance relative to hydrogen. For an accretion rate of $\dot{m} = 0.1$ Hosokawa et al. (2012a) demonstrated that deuterium shell burning starts only at protostellar masses of $\sim 80 M_\odot$ and presumably even higher masses in case of higher accretion rates. A comparison with the Eddington accretion rate in Eq. (1) thus shows that the luminosity from deuterium shell burning never becomes dominant in this mass range but in fact becomes increasingly relevant for larger masses.

It is also clear that deuterium shell burning is not going to occur close to the outer surface where the characteristic temperature for a given mass shell scales as $T \propto GM/R$. We note that from Eq. (10) $GM/R \propto t = M/\dot{M}$ at times $t \gg M/\dot{M}$ in this regime the central temperature is almost spatially constant consistent with the results of Hosokawa et al. (2012a) but a ready consideration larger than the deuterium burn temperature of $\sim 10^6$ K. Deuterium burn thus occurs when the first term in Eq. (10) is still relevant. From Fig. 1 it is evident that the radius of the shell changes considerably in that regime where the mass in the shell is almost unchanged. Adopting a scaling relation of $T \propto GM/R$ with a most constant M implies that the radius has to change by 2-3 orders of magnitude for the atmospheric temperature of 5000 K to increase to a value above 10^6 K. We therefore expect that the radius of deuterium burning correspond to a fixed fraction of the protostellar radius as long as the protostellar main sequence is not reached. From a comparison with Hosokawa et al. (2012a) at a stellar mass of $1000 M_\odot$ we obtain the normalization of this relation to be

$$R_D = 10 R_\odot \left(\frac{M}{M_\odot} \right)^{1/3}. \quad (\text{A } 2)$$

As long as the protostar remains on the Hayashi track the deuterium burning shell will not be able to move to the atmosphere and therefore it does not have an impact on the evolution of the protostar.

Appendix A.2: The pp-cycle

We consider first the energy production in the nuclear core via the pp-cycle as the composition of the star is not a

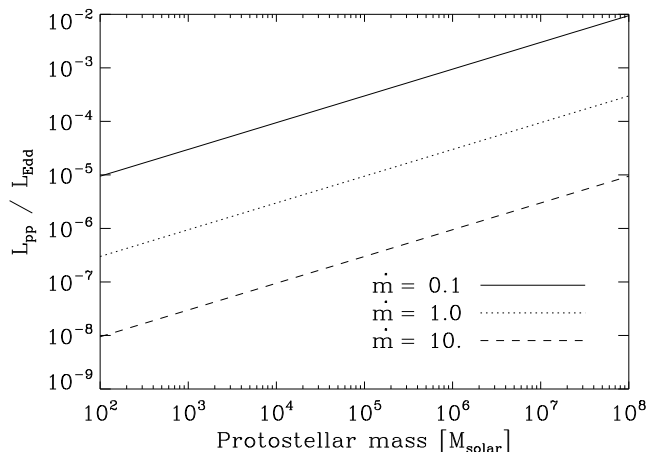


Fig. A.1. The ratio of nuclear luminosity provided via the pp-cycle (A.4) over the Eddington luminosity of the star (A.5) as a function of protostellar mass for different mass accretion rates. Larger accretion times imply that less time was available for contraction, thus reduced nuclear luminosities.

primordial. As shown by Hosokawa et al. (2012a) the typical temperature in the core is $\sim 10^8$ K and the nuclear density ~ 1 g cm $^{-3}$. We adopt here the expression of Padmanabhan (2000) for the energy production rate noting that

$$\epsilon_{pp} = \frac{2.4 \times 10^4 \rho X^2}{T_9^{2/3}} e^{-3.38/T_9^{1/3}} \text{ erg s}^{-1} \text{ g}^{-1}, \quad (\text{A } 3)$$

here T_9 denotes the temperature in units of 10^9 K and $X \sim 0.75$ the mass fraction of hydrogen. In the pp-cycle considered here has only a moderate temperature dependence. We note that the NO cycle scales as T^{20} around temperatures of 10^6 K and the triple- α process as T^{40} around temperatures of 10^8 K. For the latter cases we thus need to take into account the higher temperatures than in the center of the core as they substantially contribute to the energy production via nuclear burning. Note that $\rho_{nuc} \sim 1$ g cm $^{-3}$ and $T_9 = 0.1$ we have $\epsilon_{pp} = 43$ erg g $^{-1}$ s $^{-1}$. The luminosity provided by the pp-cycle is then given as

$$L_{pp} = \epsilon_{pp} M_{nuc} = 21.5 t_{710}^{3/2} L_{\odot}. \quad (\text{A } 4)$$

For comparison the Eddington luminosity of the protostar is given as

$$L_{\text{Edd}} = 3.8 \times 10^4 \dot{M} t L_{\odot} = 2.7 \times 10^7 \dot{m} t_{710} L_{\odot}. \quad (\text{A } 5)$$

The ratio of these luminosities is given in Fig. (A.1) showing that it remains considerably smaller than unity for stellar masses up to $10^8 M_{\odot}$. Equating the two expressions we find that the luminosity resulting from the pp-burning is relevant only at very late times $t_{pp} = 1.1 \times 10^{15}$ yr.

For practical accretion rates of $\dot{m} = 10^{-3} - 10$ and protostellar masses between $10^3 - 10^8 M_{\odot}$ the contribution from the pp-chain is never relevant and can thus be neglected for the overall evolution of the stars.

We now estimate the amount of helium produced in the core. During one fusion event an average energy of

4.3×10^{-5} erg is released implying a helium production rate of

$$\dot{N}_{\text{He,pp}} = \frac{L_{pp}}{4.3 \times 10^{-5} \text{ erg}}. \quad (\text{A } 6)$$

The helium mass in the core thus evolves as

$$\dot{M}_{\text{He,pp}} = 4m_p \times \dot{N}_{\text{He,pp}}. \quad (\text{A } 7)$$

An integration yields

$$M_{\text{He,pp}} = 6.0 \times 10^{-8} t_{710}^{5/2} M_{\odot}. \quad (\text{A } 8)$$

Equating the resulting mass with the total mass in the core a helium core can be expected after a time of 1.2×10^{10} yr. In summary when only the pp-cycle is considered nuclear burning is rather inefficient and never going to have a significant impact on the evolution of the star. However, we show in the next subsection that a transition to the NO-cycle should be expected and the implications of nuclear burning then become more relevant.